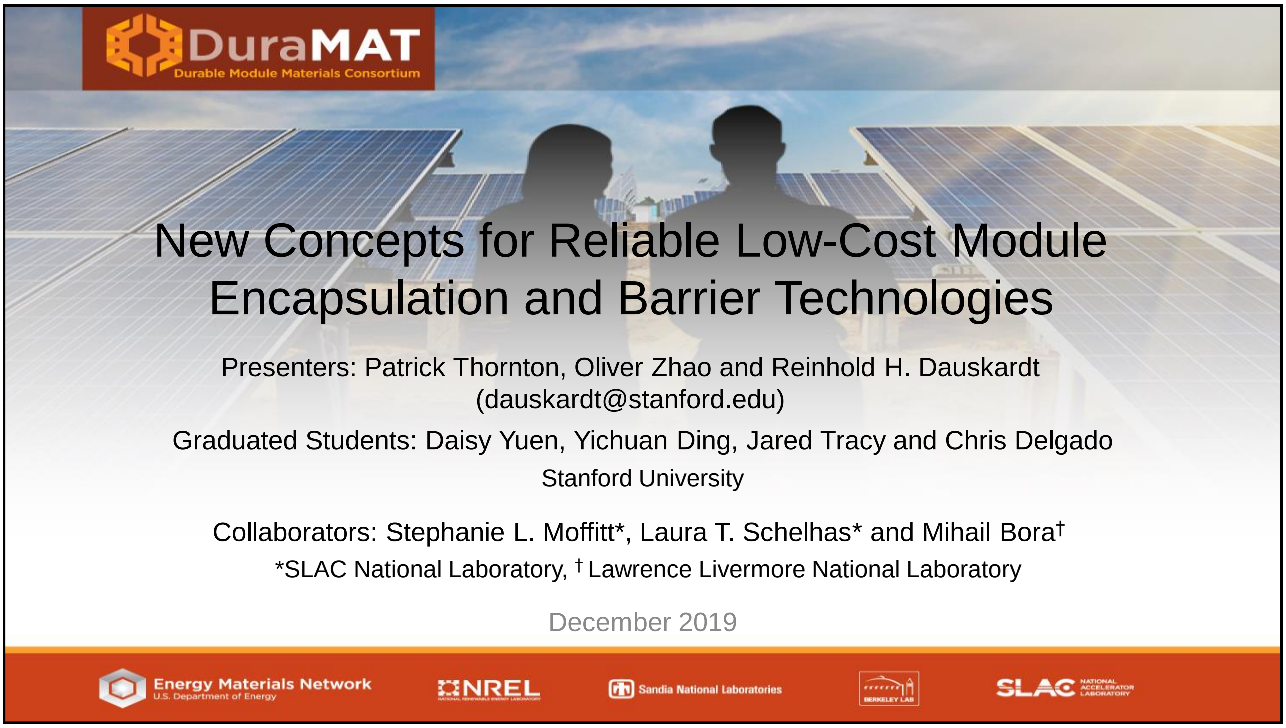

New Concepts for Reliable Low-Cost Module Encapsulation and Barrier Technologies

Presenters: Patrick Thornton, Oliver Zhao and Reinhold H. Dauskardt
(dauskardt@stanford.edu)
Graduated Students: Daisy Yuen, Yichuan Ding, Jared Tracy and Chris Delgado
Stanford University

Collaborators: Stephanie L. Moffitt*, Laura T. Schelhas* and Mihail Bora†
*SLAC National Laboratory, † Lawrence Livermore National Laboratory

December 2019

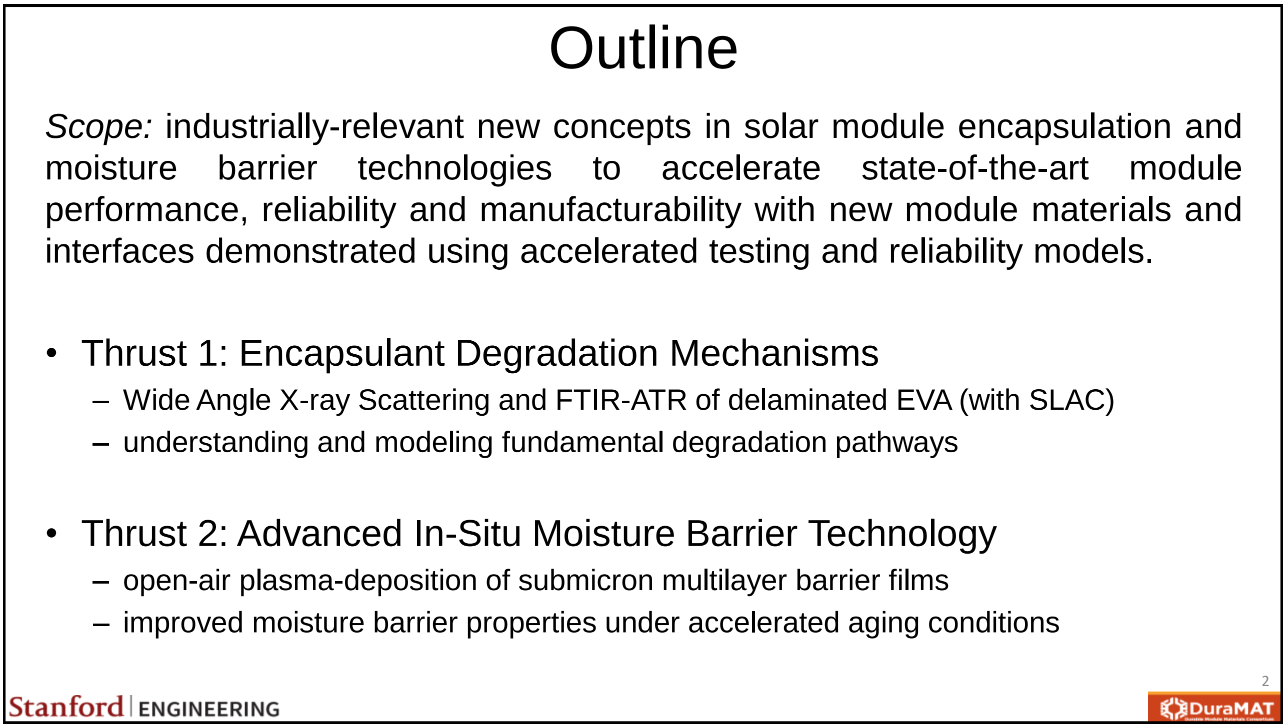

Outline

Scope: industrially-relevant new concepts in solar module encapsulation and moisture barrier technologies to accelerate state-of-the-art module performance, reliability and manufacturability with new module materials and interfaces demonstrated using accelerated testing and reliability models.

- Thrust 1: Encapsulant Degradation Mechanisms
  - Wide Angle X-ray Scattering and FTIR-ATR of delaminated EVA (with SLAC)
  - understanding and modeling fundamental degradation pathways
- Thrust 2: Advanced In-Situ Moisture Barrier Technology
  - open-air plasma-deposition of submicron multilayer barrier films
  - improved moisture barrier properties under accelerated aging conditions

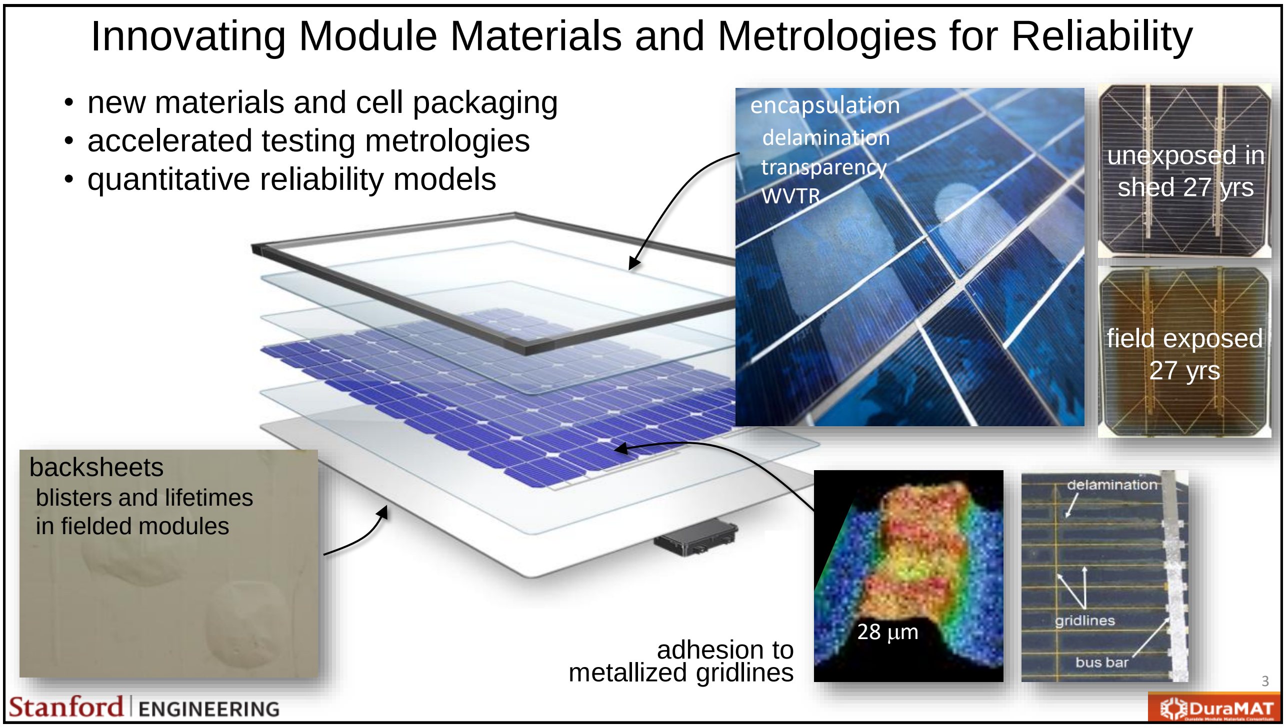

Innovating Module Materials and Metrologies for Reliability

- new materials and cell packaging
- accelerated testing metrologies
- quantitative reliability models

encapsulation
delamination
transparency
WVTR

unexposed in shed 27 yrs

field exposed 27 yrs

backsheets
blisters and lifetimes in fielded modules

adhesion to metallized gridlines

Stanford | ENGINEERING

DuraMAT

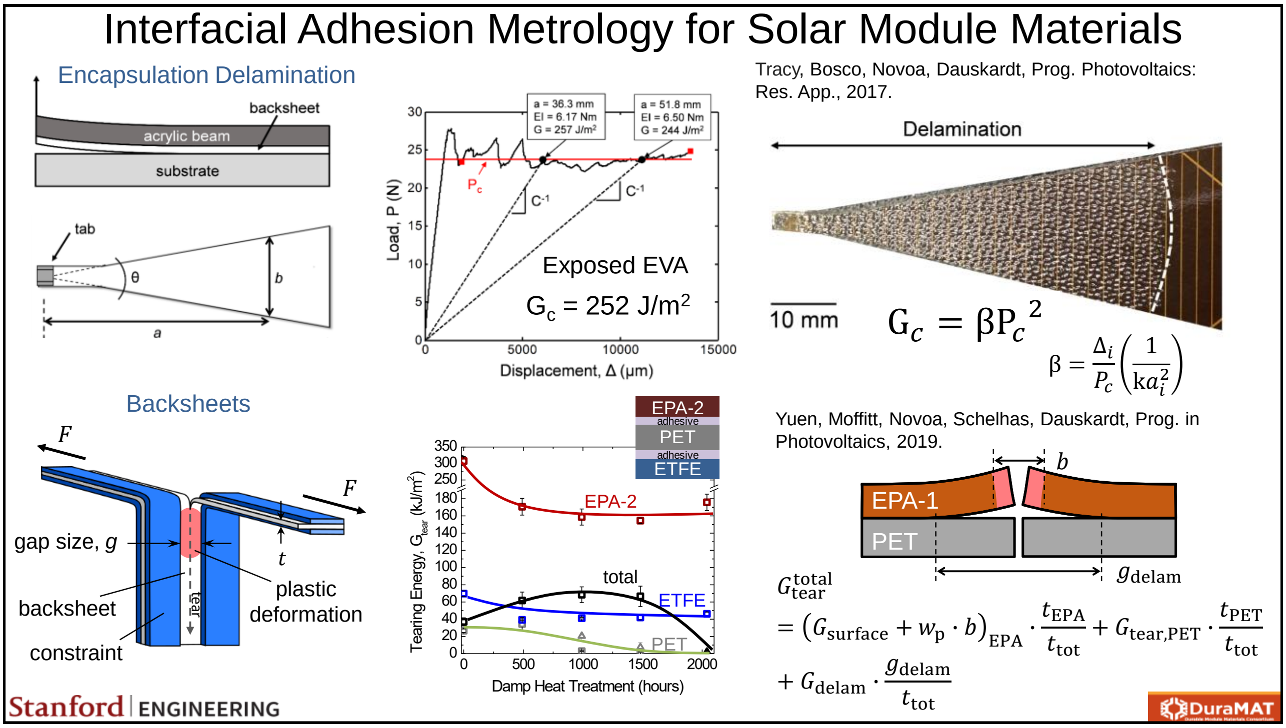

Interfacial Adhesion Metrology for Solar Module Materials

Encapsulation Delamination

Exposed EVA

$G_c = 252\ \text{J/m}^2$

Tracy, Bosco, Novoa, Dauskardt, Prog. Photovoltaics: Res. App., 2017.

$$G_c = \beta P_c^{\,2}$$

$$\beta = \frac{\Delta_i}{P_c}\left(\frac{1}{k a_i^2}\right)$$

Backsheets

Yuen, Moffitt, Novoa, Schelhas, Dauskardt, Prog. in Photovoltaics, 2019.

$$G_{\text{tear}}^{\text{total}} = \left(G_{\text{surface}} + w_{\text{p}} \cdot b\right)_{\text{EPA}} \cdot \frac{t_{\text{EPA}}}{t_{\text{tot}}} + G_{\text{tear,PET}} \cdot \frac{t_{\text{PET}}}{t_{\text{tot}}} + G_{\text{delam}} \cdot \frac{g_{\text{delam}}}{t_{\text{tot}}}$$

Stanford | ENGINEERING

DuraMAT

dauskardt@stanford.edu

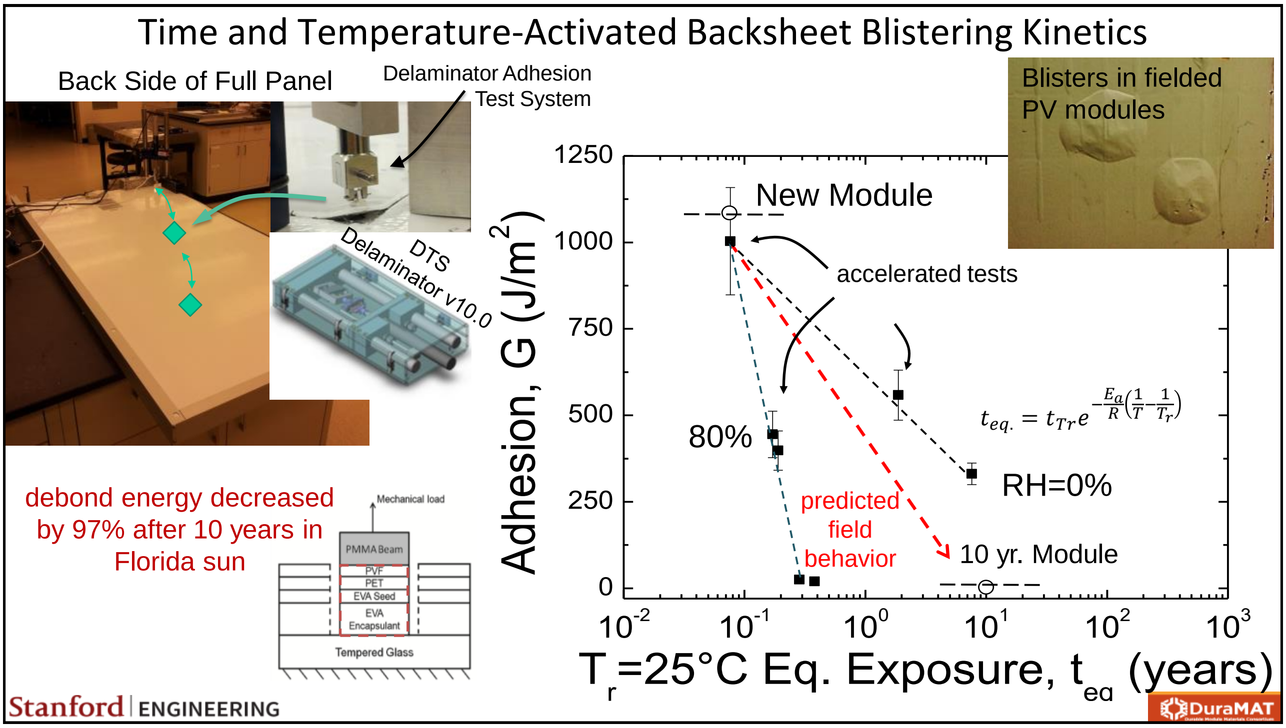

Time and Temperature-Activated Backsheet Blistering Kinetics

$$t_{eq.} = t_{Tr} e^{-\frac{E_a}{R}\left(\frac{1}{T}-\frac{1}{T_r}\right)}$$

debond energy decreased by 97% after 10 years in Florida sun

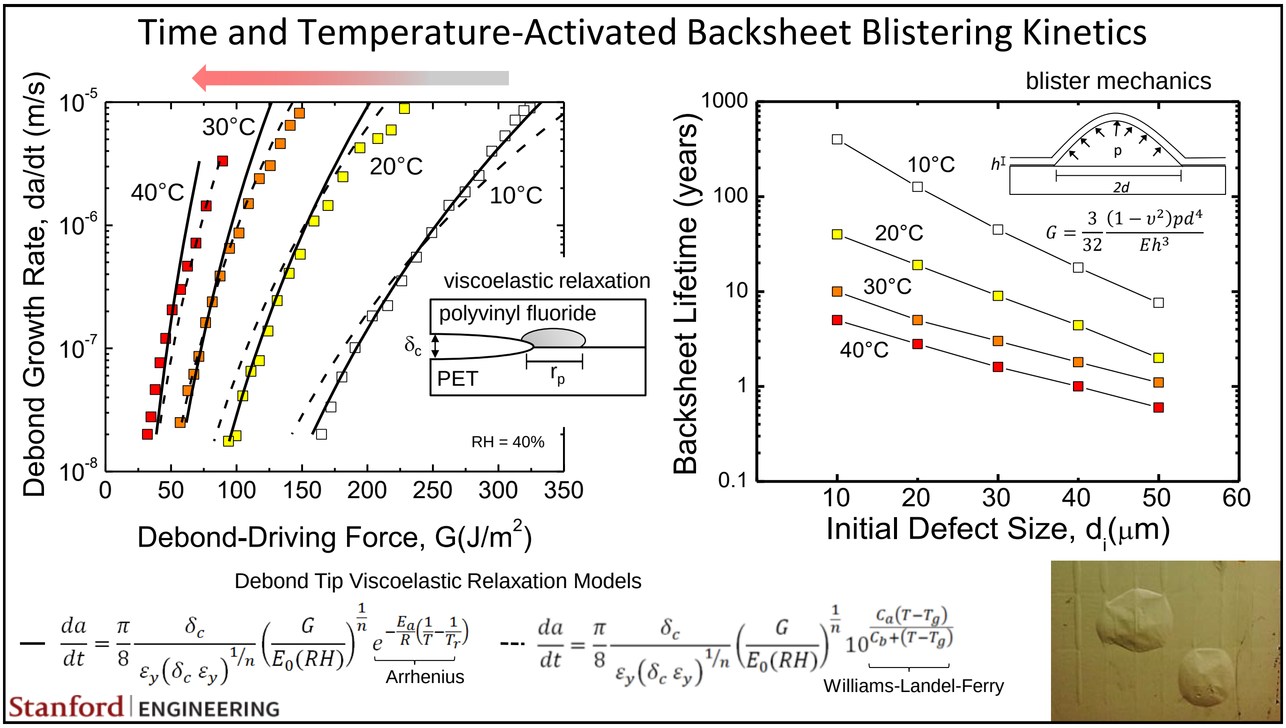

Time and Temperature-Activated Backsheet Blistering Kinetics

$$G = \frac{3}{32}\frac{(1-\nu^2)pd^4}{Eh^3}$$

Debond Tip Viscoelastic Relaxation Models

$$— \quad \frac{da}{dt} = \frac{\pi}{8}\frac{\delta_c}{\varepsilon_y(\delta_c\,\varepsilon_y)^{1/n}}\left(\frac{G}{E_0(RH)}\right)^{\frac{1}{n}} \underbrace{e^{-\frac{E_a}{R}\left(\frac{1}{T}-\frac{1}{T_r}\right)}}_{\text{Arrhenius}}$$

$$--- \quad \frac{da}{dt} = \frac{\pi}{8}\frac{\delta_c}{\varepsilon_y(\delta_c\,\varepsilon_y)^{1/n}}\left(\frac{G}{E_0(RH)}\right)^{\frac{1}{n}} \underbrace{10^{\frac{C_a(T-T_g)}{C_b+(T-T_g)}}}_{\text{Williams-Landel-Ferry}}$$

dauskardt@stanford.edu

Time and Temperature-Activated Backsheet Blistering Kinetics

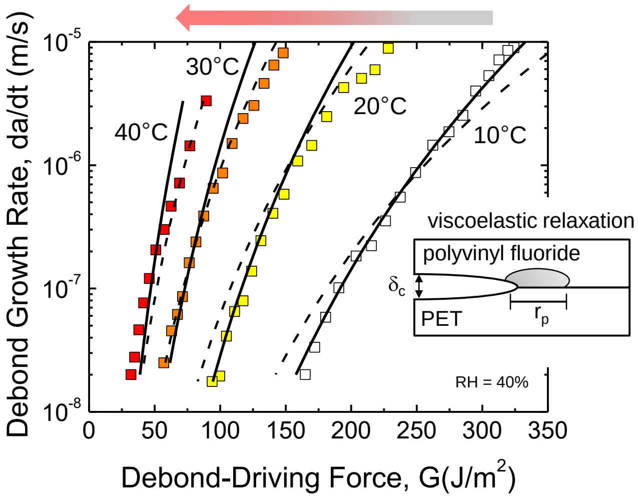

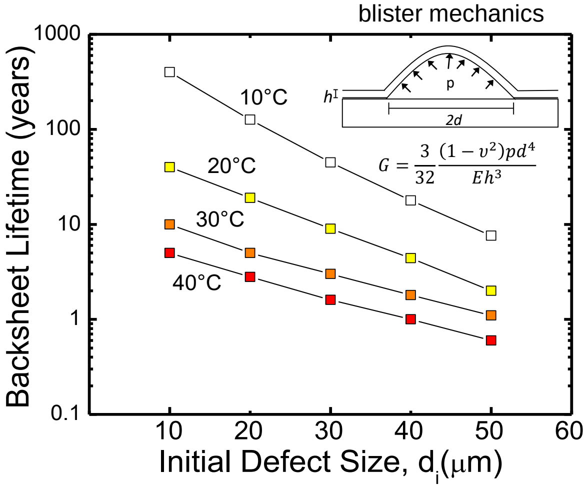

Fernando D. Novoa, David C. Miller and Reinhold H. Dauskardt, “Environmental Mechanisms of Debonding in Photovoltaic Backsheets,” **Solar Energy Materials and Solar Cells**, 120A, 87-93, 2014.

Degradation Mechanisms of Bulk Encapsulant and Interfaces

synergistic environmental stressors:

- sunlight (UV)
- heat
- humidity
- electrical bias (ion migation)
- thermomechanical strains

$G_c \approx$ 1,750 J/m² to 250 (27 yrs)

…or to 1,170 (27 yrs no UV)

What are the detailed encapsulation degradation mechanisms?

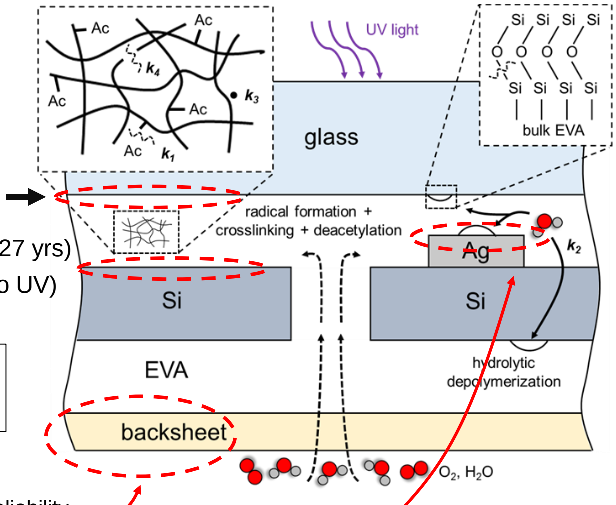

Yuen, Moffitt, Novoa, Schelhas, Dauskardt, “Tearing and reliability of photovoltaic module backsheets,” **Prog. Photovoltaics**, 2019.

Tracy, Bosco, Dauskardt, “Evaluation of Encapsulant Adhesion to Surface Metallization of Photovoltaic Cells,” **IEEE J. Photovoltaics**, 2017.

Degradation Mechanisms of Bulk Encapsulant and Interfaces

synergistic environmental stressors:

- sunlight (UV)
- heat
- humidity
- electrical bias (ion migation)
- thermomechanical strains

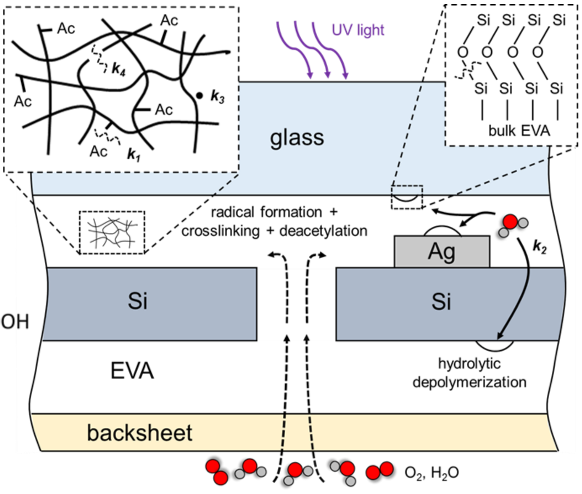

specific EVA degradation reactions:

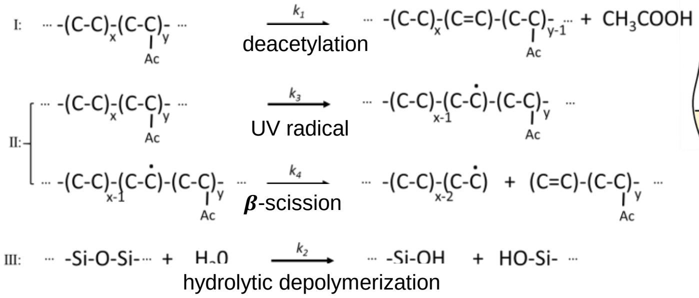

I: $\cdots\text{-(C-C)}_x\text{-(}\text{C-}\underset{\text{Ac}}{\underset{|}{\text{C}}}\text{)}_y\text{-}\cdots \xrightarrow[\text{deacetylation}]{k_1} \cdots\text{-(C-C)}_x\text{-(C=C)-(C-}\underset{\text{Ac}}{\underset{|}{\text{C}}}\text{)}_{y-1}\text{-}\cdots + CH_3COOH$

II: $\cdots\text{-(C-C)}_x\text{-(C-}\underset{\text{Ac}}{\underset{|}{\text{C}}}\text{)}_y\text{-}\cdots \xrightarrow[\text{UV radical}]{k_3} \cdots\text{-(C-C)}_{x-1}\text{-(C-}\dot{\text{C}}\text{)-(C-}\underset{\text{Ac}}{\underset{|}{\text{C}}}\text{)}_y\text{-}\cdots$

$\cdots\text{-(C-C)}_{x-1}\text{-(C-}\dot{\text{C}}\text{)-(C-}\underset{\text{Ac}}{\underset{|}{\text{C}}}\text{)}_y\text{-}\cdots \xrightarrow[\boldsymbol{\beta}\text{-scission}]{k_4} \cdots\text{-(C-C)}_{x-2}\text{-(C-}\dot{\text{C}}\text{)} + \text{(C=C)-(C-}\underset{\text{Ac}}{\underset{|}{\text{C}}}\text{)}_y\text{-}\cdots$

III: $\cdots\text{-Si-O-Si-}\cdots + H_2O \xrightarrow[\text{hydrolytic depolymerization}]{k_2} \cdots\text{-Si-OH} + \text{HO-Si-}\cdots$

Stanford | ENGINEERING

Tracy, D'hooge, Bosco, Delgado, Dauskardt, Prog. in Photovoltaics, 2018.

DuraMAT

Degradation Mechanisms of Bulk Encapsulant and Interfaces

analytical adhesion mechanics model

$$G_c(t) = \underbrace{\sum_{i}^{n} G_{c,intr,i}(t)}_{\text{intrinsic contribution}} + \underbrace{G_{c,PL}(t)}_{\text{non-linear contribution}}$$

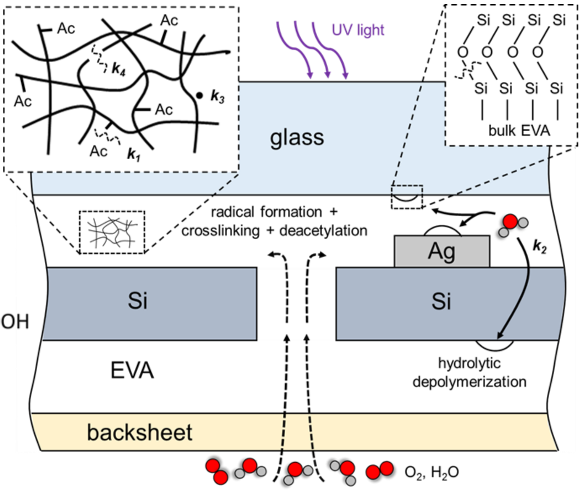

specific EVA degradation reactions:

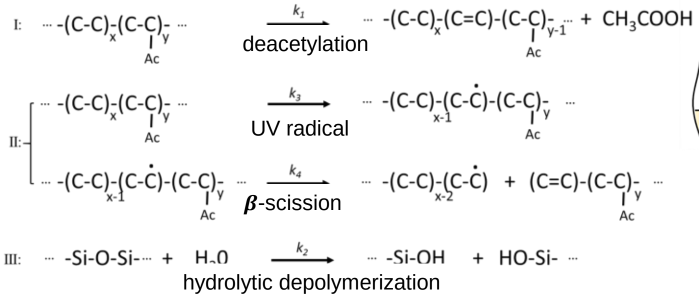

I: $\cdots\text{-(C-C)}_x\text{-(}\text{C-}\underset{\text{Ac}}{\underset{|}{\text{C}}}\text{)}_y\text{-}\cdots \xrightarrow[\text{deacetylation}]{k_1} \cdots\text{-(C-C)}_x\text{-(C=C)-(C-}\underset{\text{Ac}}{\underset{|}{\text{C}}}\text{)}_{y-1}\text{-}\cdots + CH_3COOH$

II: $\cdots\text{-(C-C)}_x\text{-(C-}\underset{\text{Ac}}{\underset{|}{\text{C}}}\text{)}_y\text{-}\cdots \xrightarrow[\text{UV radical}]{k_3} \cdots\text{-(C-C)}_{x-1}\text{-(C-}\dot{\text{C}}\text{)-(C-}\underset{\text{Ac}}{\underset{|}{\text{C}}}\text{)}_y\text{-}\cdots$

$\cdots\text{-(C-C)}_{x-1}\text{-(C-}\dot{\text{C}}\text{)-(C-}\underset{\text{Ac}}{\underset{|}{\text{C}}}\text{)}_y\text{-}\cdots \xrightarrow[\boldsymbol{\beta}\text{-scission}]{k_4} \cdots\text{-(C-C)}_{x-2}\text{-(C-}\dot{\text{C}}\text{)} + \text{(C=C)-(C-}\underset{\text{Ac}}{\underset{|}{\text{C}}}\text{)}_y\text{-}\cdots$

III: $\cdots\text{-Si-O-Si-}\cdots + H_2O \xrightarrow[\text{hydrolytic depolymerization}]{k_2} \cdots\text{-Si-OH} + \text{HO-Si-}\cdots$

Stanford | ENGINEERING

Tracy, D'hooge, Bosco, Delgado, Dauskardt, Prog. in Photovoltaics, 2018.

DuraMAT

dauskardt@stanford.edu

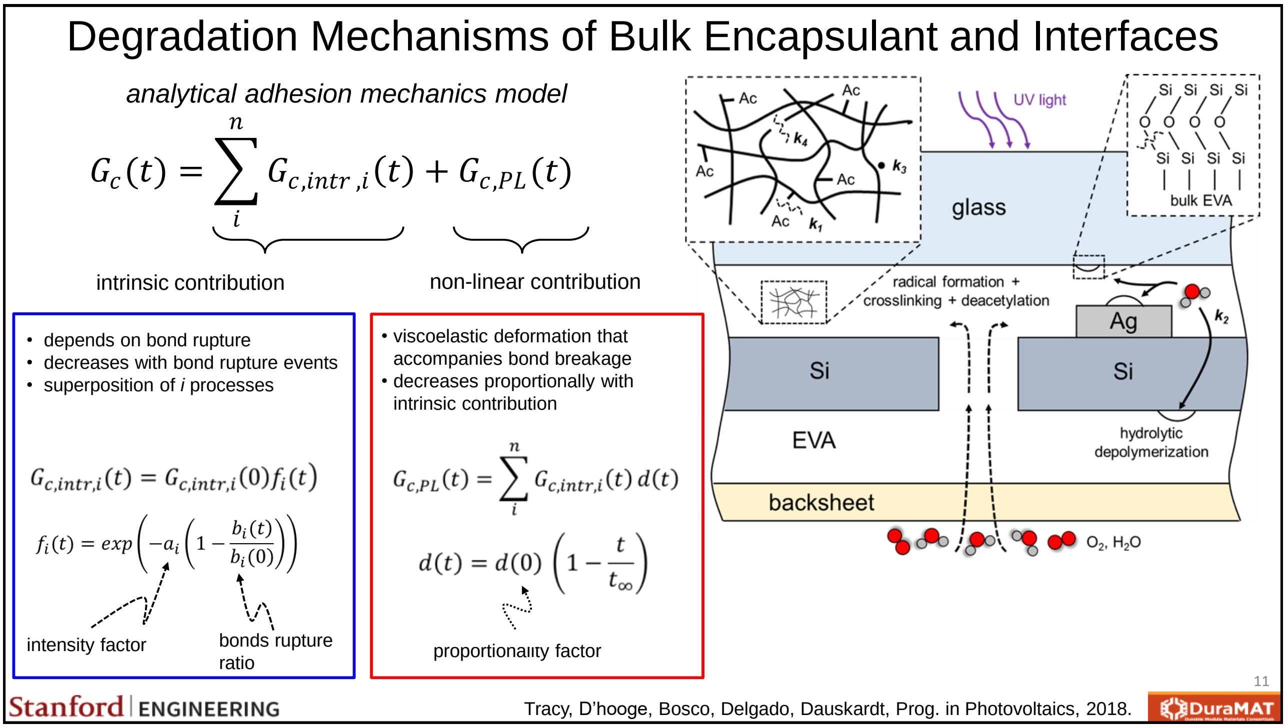

Degradation Mechanisms of Bulk Encapsulant and Interfaces

analytical adhesion mechanics model

$$G_c(t) = \underbrace{\sum_{i}^{n} G_{c,intr,i}(t)}_{\text{intrinsic contribution}} + \underbrace{G_{c,PL}(t)}_{\text{non-linear contribution}}$$

- depends on bond rupture
- decreases with bond rupture events
- superposition of *i* processes

$$G_{c,intr,i}(t) = G_{c,intr,i}(0) f_i(t)$$

$$f_i(t) = exp\left(-\overset{\text{intensity factor}}{a_i}\left(1 - \overset{\text{bonds rupture ratio}}{\frac{b_i(t)}{b_i(0)}}\right)\right)$$

intensity factor

bonds rupture ratio

- viscoelastic deformation that accompanies bond breakage
- decreases proportionally with intrinsic contribution

$$G_{c,PL}(t) = \sum_{i}^{n} G_{c,intr,i}(t)\, d(t)$$

$$d(t) = d(0)\left(1 - \frac{t}{t_\infty}\right)$$

proportionality factor

Tracy, D'hooge, Bosco, Delgado, Dauskardt, Prog. in Photovoltaics, 2018.

Stanford | ENGINEERING

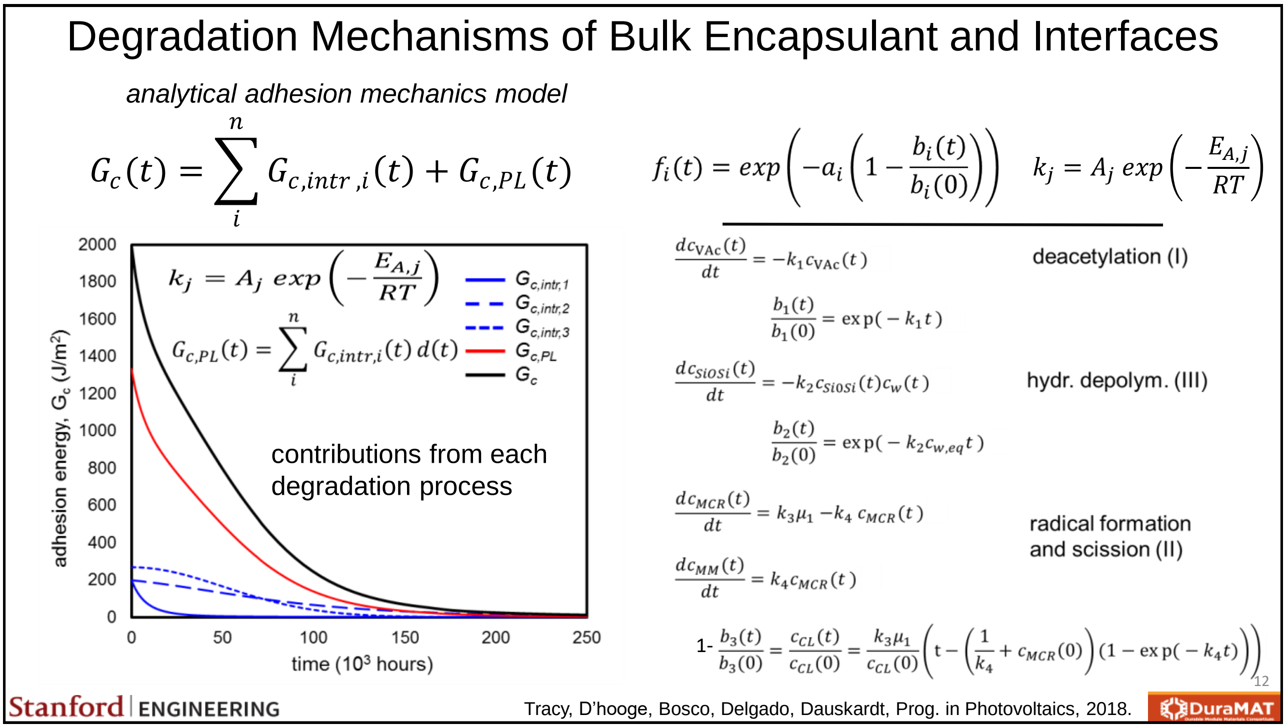

Degradation Mechanisms of Bulk Encapsulant and Interfaces

analytical adhesion mechanics model

$$G_c(t) = \sum_{i}^{n} G_{c,intr,i}(t) + G_{c,PL}(t)$$

$$f_i(t) = exp\left(-a_i\left(1 - \frac{b_i(t)}{b_i(0)}\right)\right) \quad k_j = A_j\, exp\left(-\frac{E_{A,j}}{RT}\right)$$

$$\frac{dc_{\text{VAc}}(t)}{dt} = -k_1 c_{\text{VAc}}(t)$$

deacetylation (I)

$$\frac{b_1(t)}{b_1(0)} = \exp(-k_1 t)$$

$$\frac{dc_{SiOSi}(t)}{dt} = -k_2 c_{SiOSi}(t) c_w(t)$$

hydr. depolym. (III)

$$\frac{b_2(t)}{b_2(0)} = \exp(-k_2 c_{w,eq} t)$$

$$\frac{dc_{MCR}(t)}{dt} = k_3 \mu_1 - k_4\, c_{MCR}(t)$$

$$\frac{dc_{MM}(t)}{dt} = k_4 c_{MCR}(t)$$

radical formation and scission (II)

$$1 - \frac{b_3(t)}{b_3(0)} = \frac{c_{CL}(t)}{c_{CL}(0)} = \frac{k_3 \mu_1}{c_{CL}(0)}\left(t - \left(\frac{1}{k_4} + c_{MCR}(0)\right)(1 - \exp(-k_4 t))\right)$$

Tracy, D'hooge, Bosco, Delgado, Dauskardt, Prog. in Photovoltaics, 2018.

Stanford | ENGINEERING

dauskardt@stanford.edu

Predictive Modelling for Adhesion Degradation

Sensitivity of adhesion to individual degradation processes varies temporally:

- deacetylation dominates initially
- UV radical formation and scission dominate at intermediate timeframes
- interface hydrolysis dominates at *t* >10 yrs

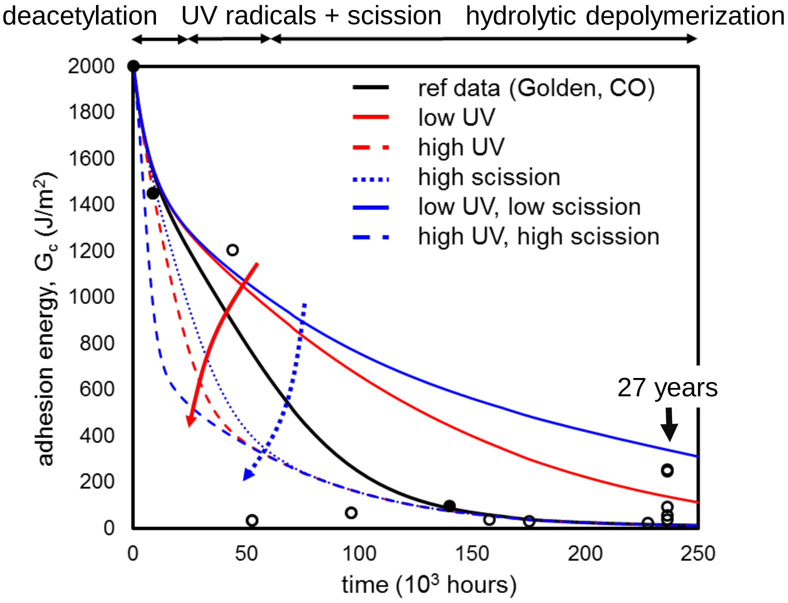

Stanford | ENGINEERING

Tracy, D'hooge, Bosco, Delgado, Dauskardt, Prog. in Photovoltaics, 2018.

DuraMAT

Predictive Modelling for Adhesion Degradation

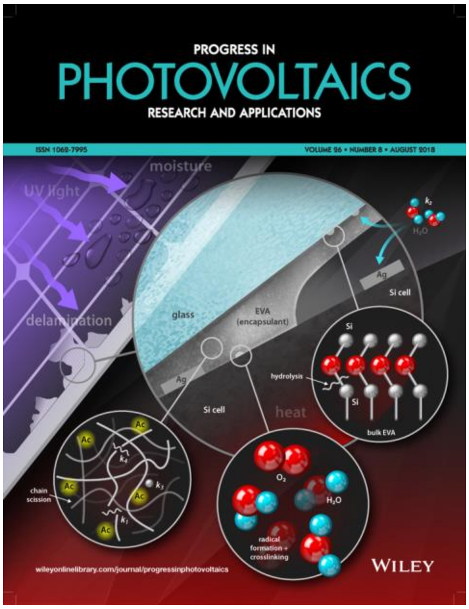

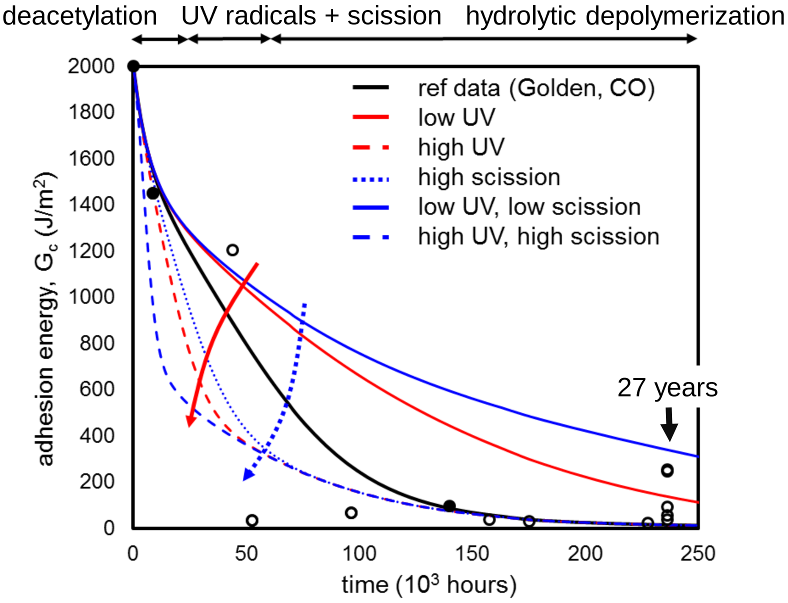

Stanford | ENGINEERING

Tracy, D'hooge, Bosco, Delgado, Dauskardt, Prog. in Photovoltaics, 2018.

DuraMAT

dauskardt@stanford.edu

Modular Description of Critical Degradation Pathways in EVA

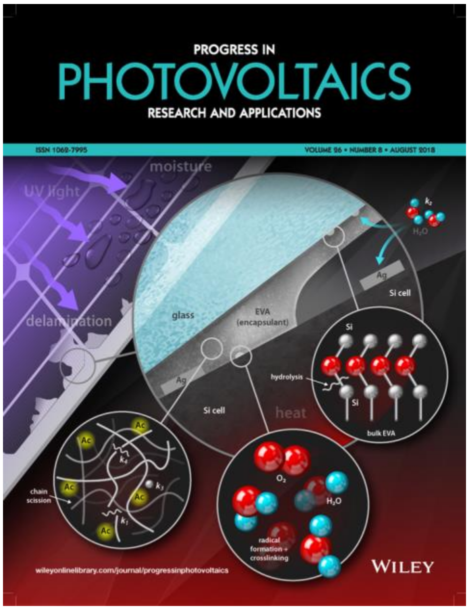

Degradation Pathways

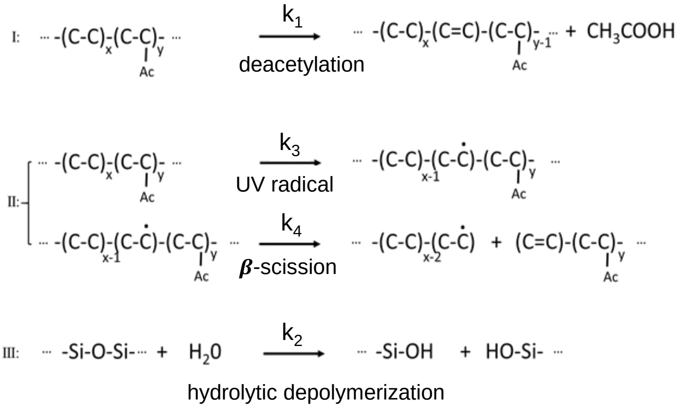

$$\text{I:}\quad \cdots\text{-(C-C)}_x\text{-}\underset{\text{Ac}}{\text{(C-C)}_y}\text{-}\cdots \xrightarrow[\text{deacetylation}]{k_1} \cdots\text{-(C-C)}_x\text{-(C=C)-}\underset{\text{Ac}}{\text{(C-C)}_{y-1}}\text{-}\cdots + CH_3COOH$$

$$\text{II:}\quad \cdots\text{-(C-C)}_x\text{-}\underset{\text{Ac}}{\text{(C-C)}_y}\text{-}\cdots \xrightarrow[\text{UV radical}]{k_3} \cdots\text{-(C-C)}_{x-1}\text{-(C-}\dot{\text{C}}\text{)-}\underset{\text{Ac}}{\text{(C-C)}_y}\text{-}\cdots$$

$$\cdots\text{-(C-C)}_{x-1}\text{-(C-}\dot{\text{C}}\text{)-}\underset{\text{Ac}}{\text{(C-C)}_y}\text{-}\cdots \xrightarrow[\beta\text{-scission}]{k_4} \cdots\text{-(C-C)}_{x-2}\text{-(C-}\dot{\text{C}}\text{)} + \text{(C=C)-}\underset{\text{Ac}}{\text{(C-C)}_y}\text{-}\cdots$$

$$\text{III:}\quad \cdots\text{-Si-O-Si-}\cdots + H_20 \xrightarrow{k_2} \cdots\text{-Si-OH} + \text{HO-Si-}\cdots$$

hydrolytic depolymerization

Stanford | ENGINEERING

DuraMAT

Advanced Characterization of EVA Degradation: WAXS

EVA is a semi-crystalline polymer…

Primary Crystalline Phases

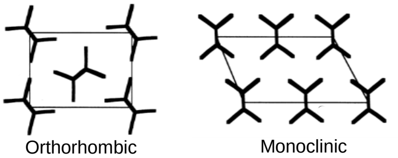

Image from Gedde & Mattozzi, *Adv.Polym Sci, 2004.*

— crystalline vol. frac. ~ 5%
— remainder amorphous

—Exposure Conditions—
10,000 Hours

”Dark” – 85˚C, 13.5%RH, No UV,

“Light” – 65˚C, 30%RH,
with UV: 81 W/m^2

Wide Angle X-ray Scattering

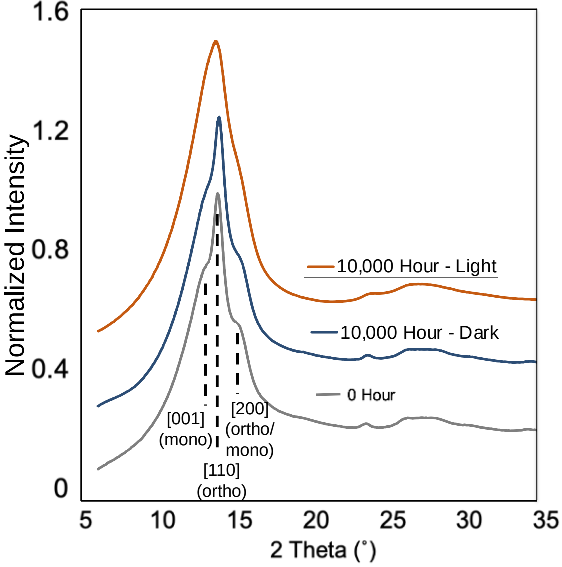

Stanford | ENGINEERING

With Laura Schelhas and Stephanie Moffitt, SLAC

DuraMAT

dauskardt@stanford.edu

Advanced Characterization of EVA Degradation: WAXS

EVA is a semi-crystalline polymer…

Primary Crystalline Phases

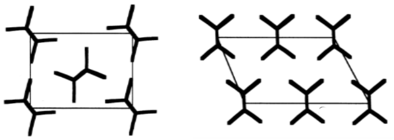

Image from Gedde & Mattozzi, *Adv.Polym Sci, 2004.*

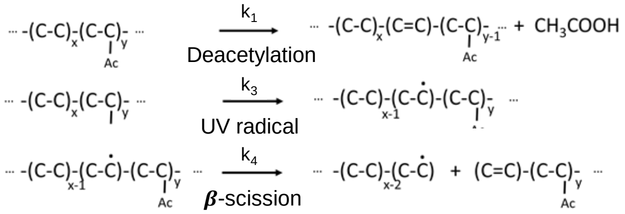

$$\cdots\text{-(C-C)}_x\text{-}\underset{\text{Ac}}{\text{(C-C)}}_y\text{-}\cdots \xrightarrow[\text{Deacetylation}]{k_1} \cdots\text{-(C-C)}_x\text{-(C=C)-}\underset{\text{Ac}}{\text{(C-C)}}_{y-1}\text{-}\cdots + CH_3COOH$$

$$\cdots\text{-(C-C)}_x\text{-}\underset{|}{\text{(C-C)}}_y\text{-}\cdots \xrightarrow[\text{UV radical}]{k_3} \cdots\text{-(C-C)}_{x-1}\text{-(C-}\dot{\text{C}}\text{)-}\underset{}{\text{(C-C)}}_y\text{-}\cdots$$

$$\cdots\text{-(C-C)}_{x-1}\text{-(C-}\dot{\text{C}}\text{)-}\underset{\text{Ac}}{\text{(C-C)}}_y\text{-}\cdots \xrightarrow[\beta\text{-scission}]{k_4} \cdots\text{-(C-C)}_{x-2}\text{-(C-}\dot{\text{C}}\text{)} + \text{(C=C)-}\underset{\text{Ac}}{\text{(C-C)}}_y\text{-}\cdots$$

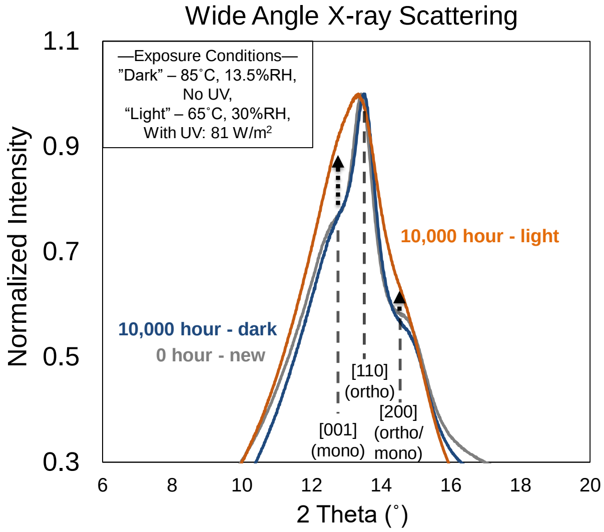

Monoclinic crystallites form from shorter ethylene segments. The comparative increase of monoclinic phase evidences main polyethylene chain degradation.

Stanford | ENGINEERING

With Laura Schelhas and Stephanie Moffitt, SLAC

DuraMAT

Advanced Characterization of EVA Degradation: FTIR-ATR

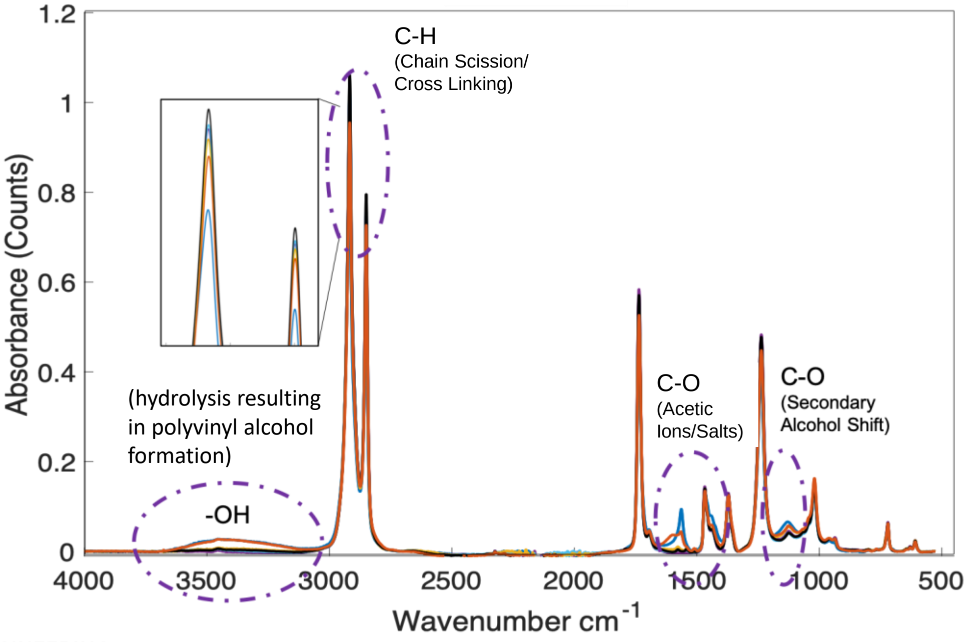

Stanford | ENGINEERING

DuraMAT

dauskardt@stanford.edu

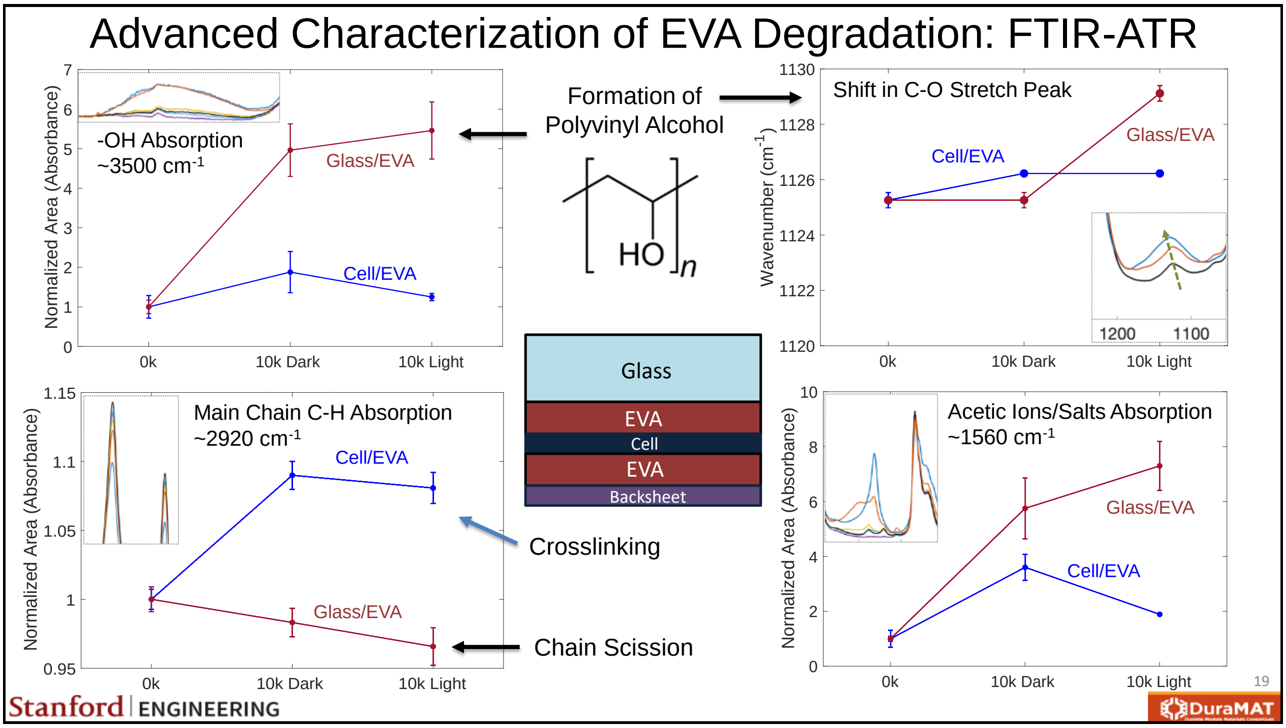

Advanced Characterization of EVA Degradation: FTIR-ATR

Formation of Polyvinyl Alcohol

Crosslinking

Chain Scission

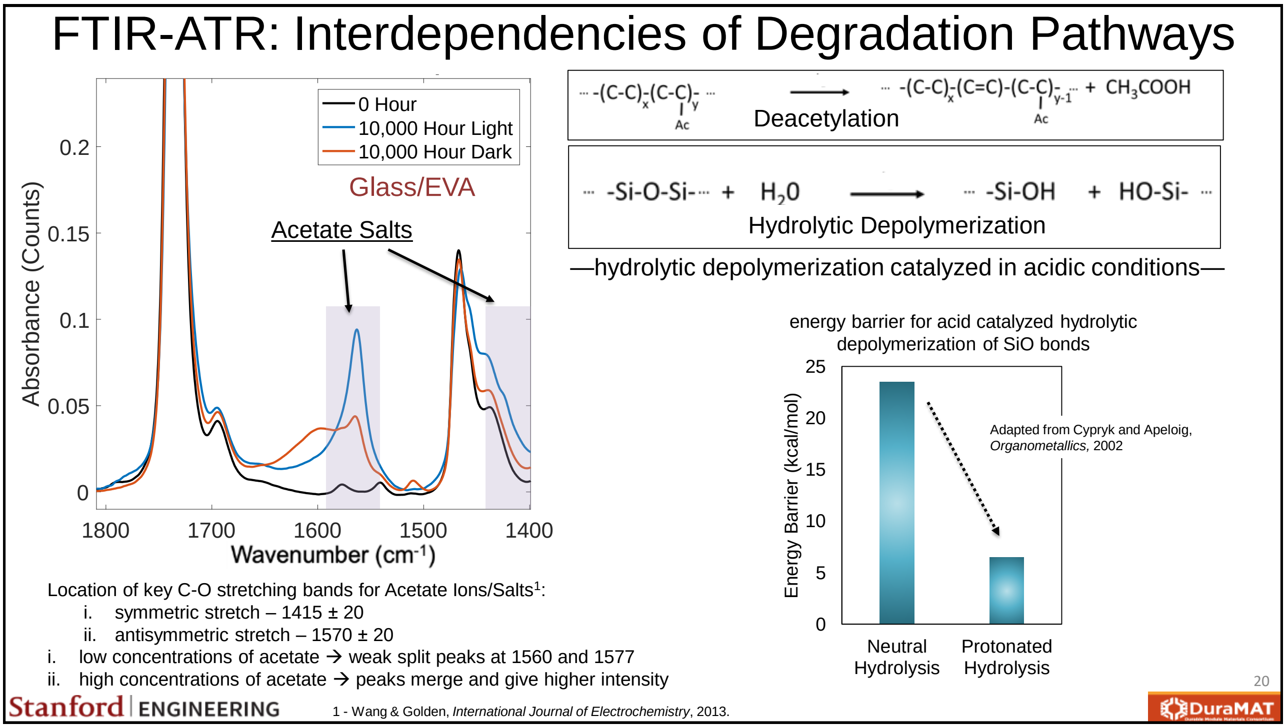

FTIR-ATR: Interdependencies of Degradation Pathways

$$\cdots\text{-(C-C)}_x\text{-}\underset{\text{Ac}}{\text{(C-C)}}_y\text{-}\cdots \longrightarrow \cdots\text{-(C-C)}_x\text{-(C=C)-}\underset{\text{Ac}}{\text{(C-C)}}_{y-1}\text{-}\cdots + CH_3COOH$$

Deacetylation

$$\cdots\text{-Si-O-Si-}\cdots + H_2 0 \longrightarrow \cdots\text{-Si-OH} + \text{HO-Si-}\cdots$$

Hydrolytic Depolymerization

—hydrolytic depolymerization catalyzed in acidic conditions—

Adapted from Cypryk and Apeloig, *Organometallics*, 2002

Location of key C-O stretching bands for Acetate Ions/Salts[1]:

  i. symmetric stretch – 1415 ± 20
  ii. antisymmetric stretch – 1570 ± 20

i. low concentrations of acetate → weak split peaks at 1560 and 1577
ii. high concentrations of acetate → peaks merge and give higher intensity

1 - Wang & Golden, *International Journal of Electrochemistry*, 2013.

dauskardt@stanford.edu

FTIR-ATR: Interdependencies of Degradation Pathways

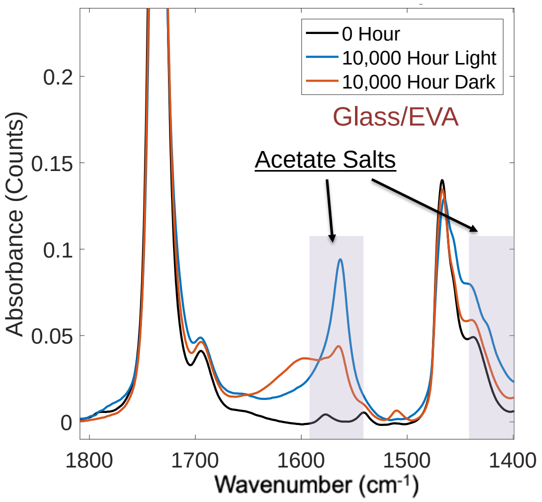

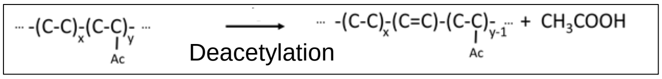

$$\cdots\text{-(C-C)}_x\text{-}\underset{\text{Ac}}{\text{(C-C)}}_y\text{-}\cdots \xrightarrow{\text{Deacetylation}} \cdots\text{-(C-C)}_x\text{-(C=C)-}\underset{\text{Ac}}{\text{(C-C)}}_{y-1}\text{-}\cdots + CH_3COOH$$

$\cdots$ -Si-O-Si- $\cdots$ + H_2O $\longrightarrow$ $\cdots$ -Si-OH + HO-Si- $\cdots$

Hydrolytic Depolymerization

—hydrolytic depolymerization catalyzed in acidic conditions—

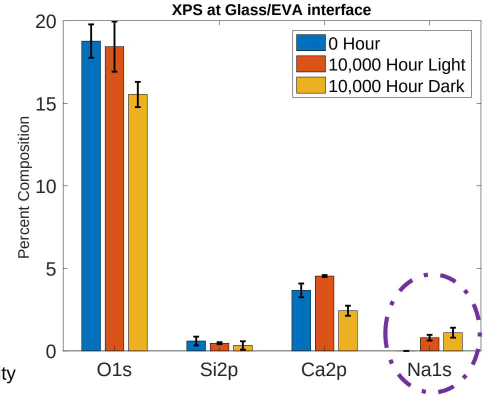

Location of key C-O stretching bands for Acetate Ions/Salts[1]:
   i. symmetric stretch – 1415 ± 20
   ii. antisymmetric stretch – 1570 ± 20

i. low concentrations of acetate → weak split peaks at 1560 and 1577
ii. high concentrations of acetate → peaks merge and give higher intensity

FTIR-ATR: Interdependencies of Degradation Pathways

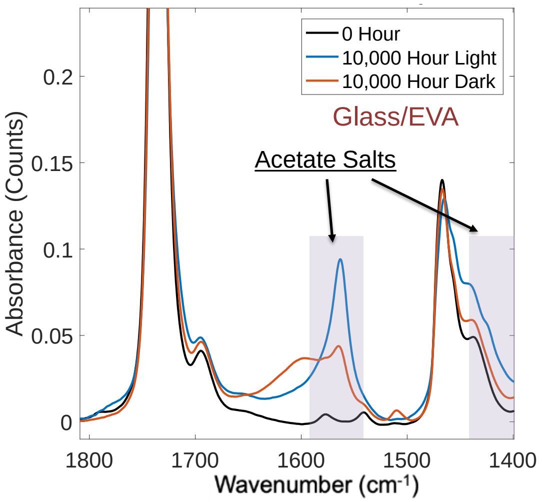

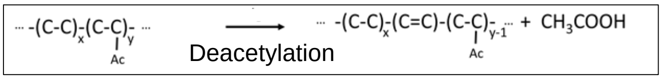

$$\cdots\text{-(C-C)}_x\text{-}\underset{\text{Ac}}{\text{(C-C)}}_y\text{-}\cdots \xrightarrow{\text{Deacetylation}} \cdots\text{-(C-C)}_x\text{-(C=C)-}\underset{\text{Ac}}{\text{(C-C)}}_{y-1}\text{-}\cdots + CH_3COOH$$

$\cdots$ -Si-O-Si- $\cdots$ + H_2O $\longrightarrow$ $\cdots$ -Si-OH + HO-Si- $\cdots$

Hydrolytic Depolymerization

—hydrolytic depolymerization catalyzed in acidic conditions—

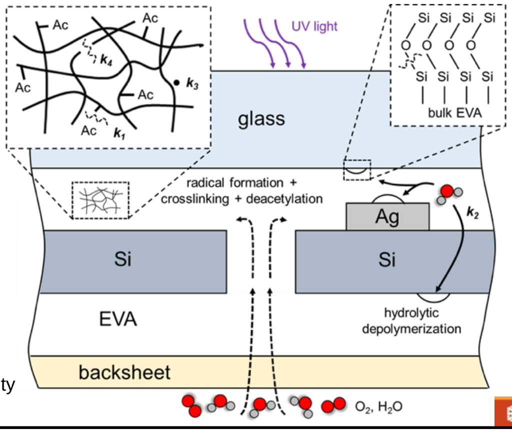

Location of key C-O stretching bands for Acetate Ions/Salts[1]:
   i. symmetric stretch – 1415 ± 20
   ii. antisymmetric stretch – 1570 ± 20

i. low concentrations of acetate → weak split peaks at 1560 and 1577
ii. high concentrations of acetate → peaks merge and give higher intensity

dauskardt@stanford.edu

Outline

Scope: industrially-relevant new concepts in solar module encapsulation and moisture barrier technologies to accelerate state-of-the-art module performance, reliability and manufacturability with new module materials and interfaces demonstrated using accelerated testing and reliability models.

- Thrust 1: Encapsulant Degradation Mechanisms
  - Wide Angle X-ray Scattering and FTIR-ATR of delaminated EVA (with SLAC)
  - understanding and modeling of fundamental degradation pathways
- Thrust 2: Advanced In-Situ Moisture Barrier Technology
  - open-air plasma-deposition of submicron multilayer barrier films
  - improved moisture barrier properties under accelerated aging conditions

Open-Air Spray Plasma Processing of In-Situ Barrier Films

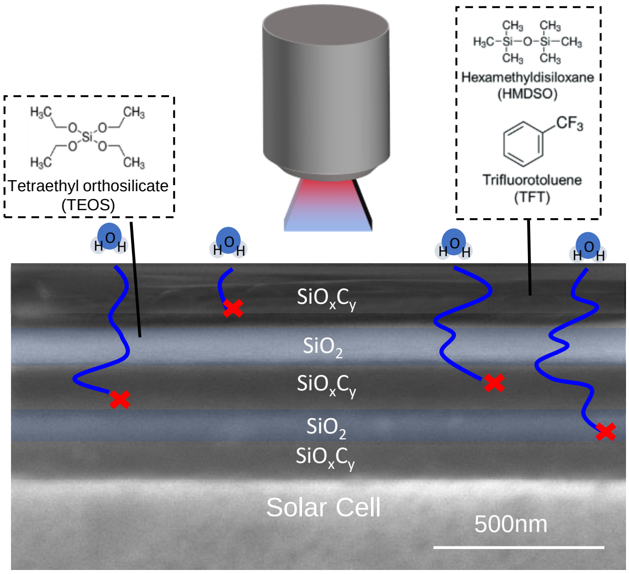

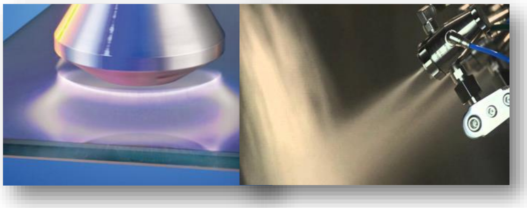

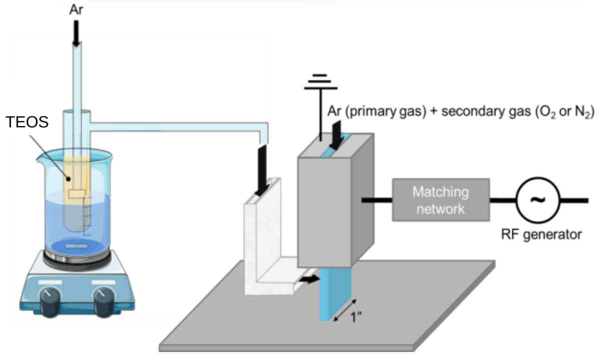

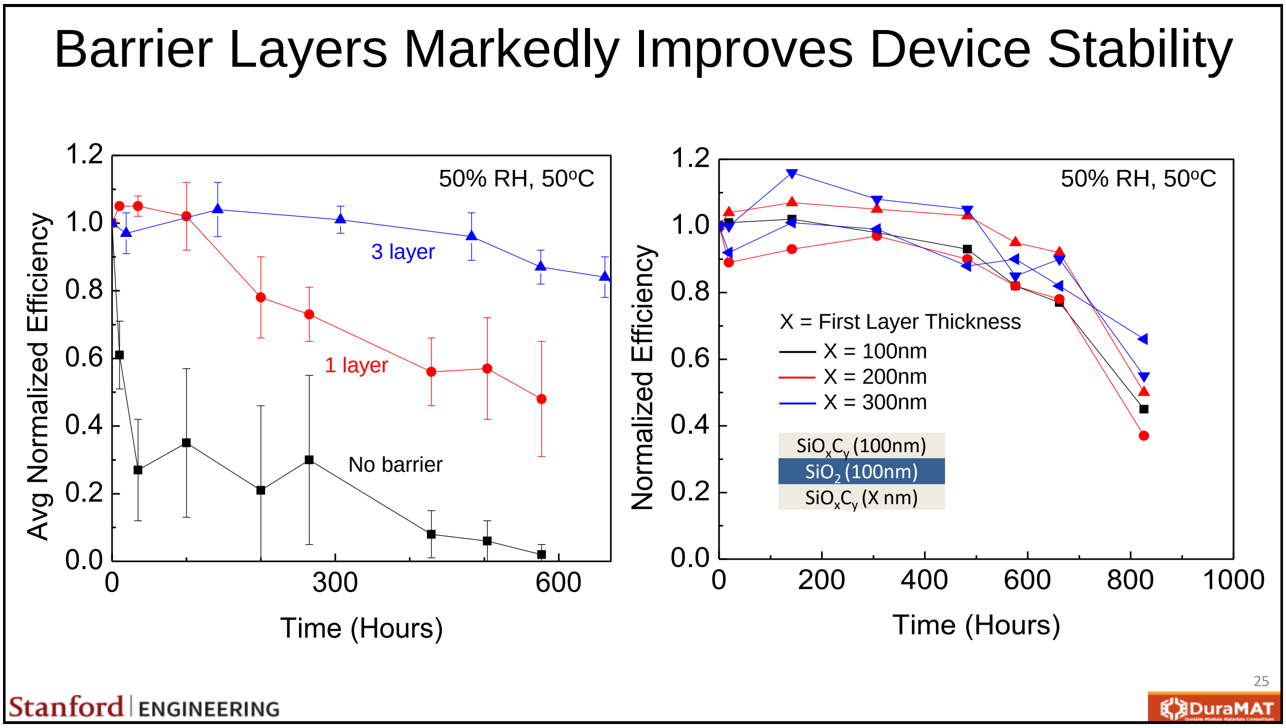

Barrier Layers Markedly Improves Device Stability

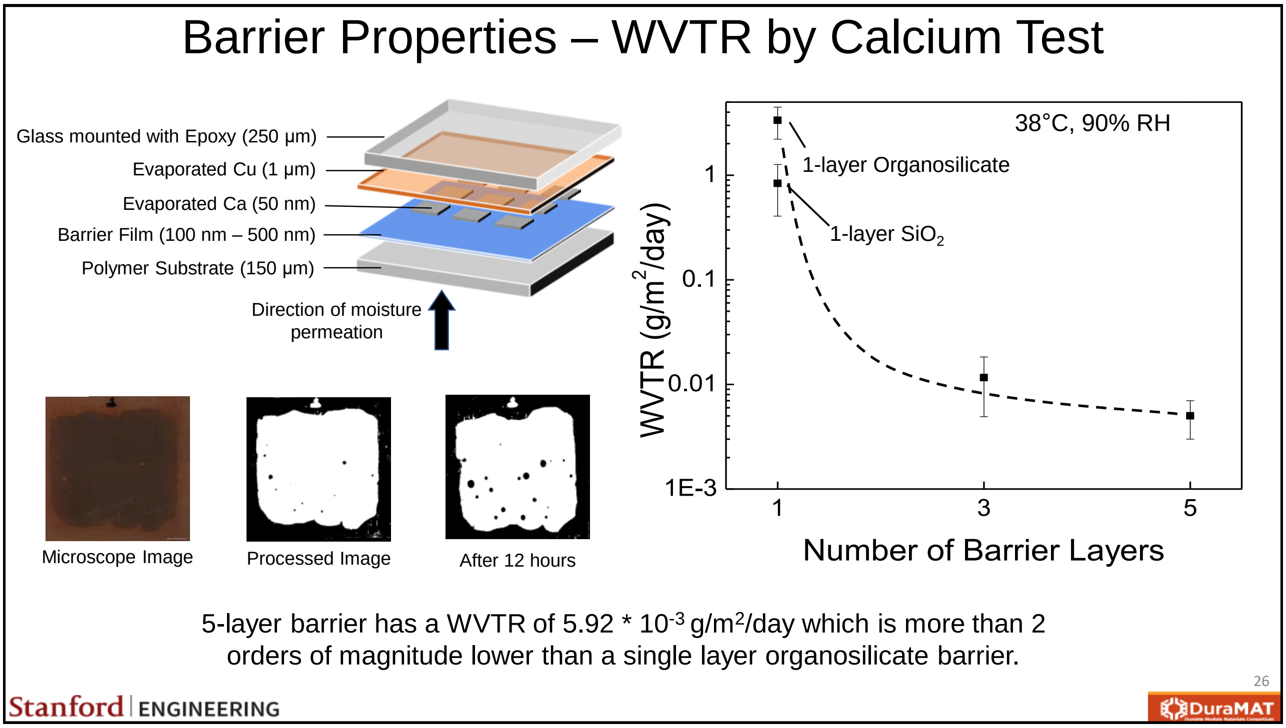

Barrier Properties – WVTR by Calcium Test

Glass mounted with Epoxy (250 μm)
Evaporated Cu (1 μm)
Evaporated Ca (50 nm)
Barrier Film (100 nm – 500 nm)
Polymer Substrate (150 μm)
Direction of moisture permeation

Microscope Image
Processed Image
After 12 hours

5-layer barrier has a WVTR of 5.92 * 10^{-3} g/m^2/day which is more than 2 orders of magnitude lower than a single layer organosilicate barrier.

dauskardt@stanford.edu

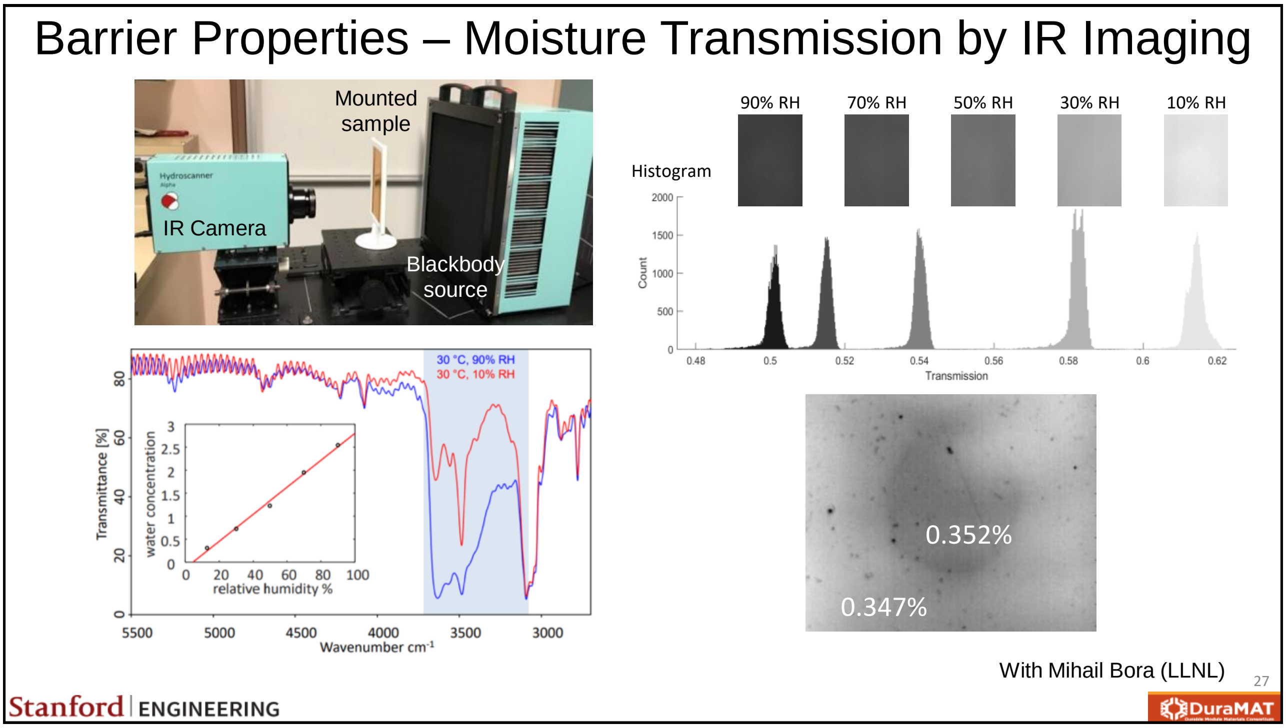

Barrier Properties – Moisture Transmission by IR Imaging

With Mihail Bora (LLNL)

Stanford | ENGINEERING

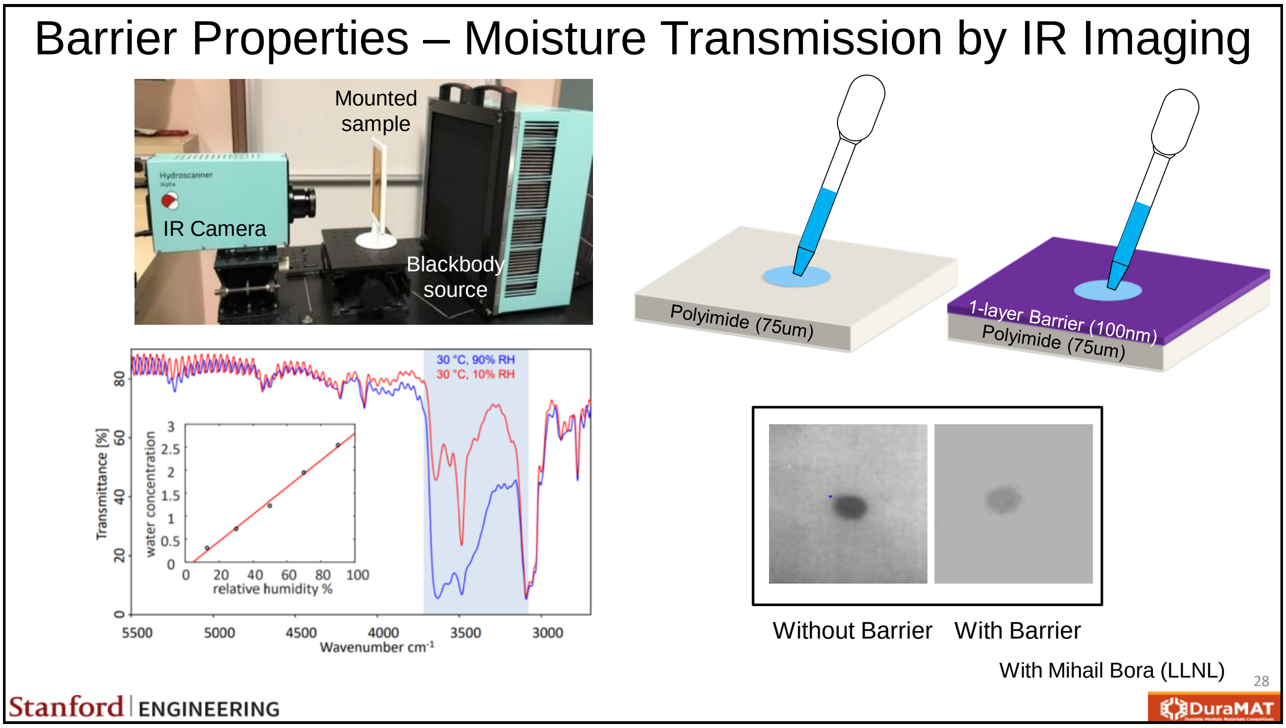

Barrier Properties – Moisture Transmission by IR Imaging

Without Barrier With Barrier

With Mihail Bora (LLNL)

Stanford | ENGINEERING

dauskardt@stanford.edu

Conclusion: New Concepts in Module Reliability

Scope: industrially-relevant new concepts in solar module encapsulation and moisture barrier technologies to accelerate state-of-the-art module performance, reliability and manufacturability with new module materials and interfaces demonstrated using accelerated testing and reliability models.

Thrust 1: Encapsulant Degradation Mechanisms

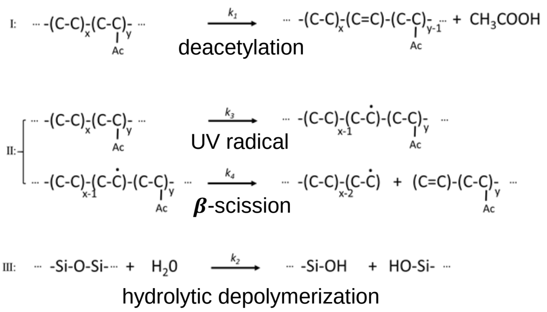

High resolution WAXS and FTIR-ATR explain the presence and interdependencies of degradation pathways.

Thrust 2: Open-air In-Situ Moisture Barriers

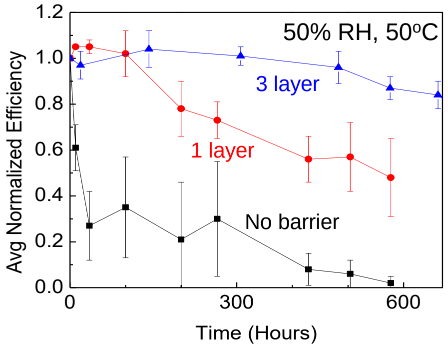

Low-cost barrier layers significantly improves solar cell stability in humid environments.

Future Directions – Advancing Bifacial Modules

Advancing Bifacial Solar Module Reliability and Manufacturability with New Module Materials and Light-Weight Transparent Back Lamination

Emergence of Bifacial PV: Bifacial panels have significant advantages over mono-facial modules with increased power yield by up to 30%, and costs for bifacial PERC production are within $0.01—0.02/W of the costs for mono-facial PERC production*.

Builds directly on capabilities developed in our current DuraMAT program, include advanced characterization and modeling of fundamental degradation pathways in module materials and our advanced in-situ moisture barrier technology.

Leverages the DuraMAT Materials Characterization and Forensics capability through our continued partnership with SLAC and collaboration with Dr. Matt Reese on WVTR characterization and Dr. Mike Woodhouse at NREL involving bifacial techno-economic analyses useful for U.S. PV manufacturing.

Thrust 1 - Bifacial module materials degradation and interface reliability characterization.

Thrust 2 – Develop and validate a transparent polymer back lamination technology comprising 1) a conformal, dense, multi-dyad thin-film barrier structure deposited directly onto the module backside using a scalable open-air spray plasma for pin-hole free barriers, 2) a high-quality transparent encapsulate, and 3) transparent polymer backsheet containing fluoropolymer which provides robust mechanical protection.

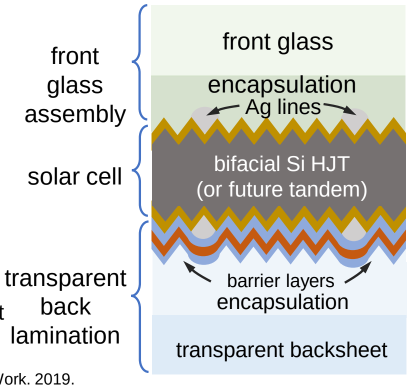

*Woodhouse, "Considerations for Utilizing Bifacial PV Technologies…" bifiPV Work. 2019.